Journal of Engineering Research and Applied Science
Available at www.journaleras.com
Volume 10 (2), December 2021, pp 1828-1842
ISSN 2147-3471 © 2021

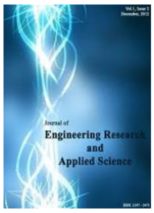

Petrological characteristics of late Cretaceous volcanic rocks of Demirören (Gümüşhane, NE Turkey) region

A.Vural[1,a], A.Kaygusuz[1], İ.Akpınar[1]

[1]Gümüşhane University, Geological Engineering, Gümüşhane, Turkey.

Accepted 1 August 2021

Abstract
Subduction-related Late Cretaceous volcanic rocks are widely observed in the northern zone of the Eastern Pontides, while their distribution in the southern zone is minimal. In this study, the petrographic and geochemical properties of Late Cretaceous volcanic rocks outcropping in Demirören (Gümüşhane) and its surroundings in the southern zone of the Eastern Pontides were investigated. These rocks are composed of basaltic andesite and andesite, and the main minerals are plagioclase, alkali feldspar, hornblende, biotite and minor augite. Volcanic rocks have calc-alkaline character and have medium to high-K content. They are enriched with light rare earth elements (LREE) and large ion lithophile elements (LILE) and depleted in high-field strenght elements (HFSE). The chondrite normalized rare earth element distributions are low to moderately enriched (La_N/Lu_N=3-12) and are concave in shape. Fractional crystallization played a major role in the development of the rocks. All data indicate that the origin magma of volcanic rocks may be derived from the partial melting of a subcontinental lithospheric mantle (SCLM), whih was enriched by fluids from a subduction of oceanic crust.

Keywords Eastern pontides, Gümüşhane, late cretaceous, whole-rock geochemistry, petrography, Demirören volcanic rocks.

1. Introduction

Eastern Pontides (NE Turkey) is one of the areas where volcanic and plutonic rocks [1–8] are widely observed and important mineral deposits are located [9–13]. Three main volcanic cycles took place in the Eastern Pontides: Liassic, Cretaceous, and Eocene (and later) [14,15]. The Eastern Pontides were divided into two zones as southern and northern zones by [16] due to the Cretaceous aged rocks differ lithologically in the southern and northern regions. The study area is located in the southern zone of the Eastern Pontides.

Many detailed studies have been carried out on the Late Cretaceous plutonic rocks in the Eastern Pontides [5, 17–19], and the studies on their volcanic equivalents are limited [20–25]. Radiometric age data for Late Cretaceous volcanic rocks in the Eastern Pontides are limited (Table 1). The ages of the Late Cretaceous volcanic rocks range from 75 to 92 Ma (Table 1).

Table 1. Crystallization ages of Late Cretaceous volcanic rocks in the Eastern Pontides (changed from [26])

Name	Rock Types	Age (Ma)	Dating	Reference
Değirmentaşı (Torul/Gümüşhane)	Dacite	77.99±3.76	K-Ar	[26]
Artvin	Rhyolite	83.04±0.39 86.51±0.35	$^{206}Pb/^{238}U$	[24]
Murgul (Artvin)	Basalt Dacite	92.1±1.2 88.8±0.9	$^{40}Ar/^{39}Ar$	[27]
Rize	Dacite	83.2±1.0	$^{40}Ar/^{39}Ar$	[28]
Akçaabat (Trabzon)	Basalt	82.61±0.34	$^{40}Ar/^{39}Ar$	[29]
Ordu	Basalt Rhyo-dacite	86.02±0.52 75.34±0.10	$^{206}Pb/^{238}U$	[22]
Tekke (Gümüşhane)	Felsic tuff	84.05±0.94 81.09±0.62	$^{206}Pb/^{238}U$	[30]

[a] Corresponding author; alaaddinvural@hotmail.com

		77.1±1.0		
Tirebolu (Giresun)	Dacite Rhyolite	91.1 ± 1.3 83.1 ± 1.5	$^{206}Pb/^{238}U$	[31]
Maden (Bayburt)	Trachy-andesite	80.9 ±0.9	$^{40}Ar/^{39}Ar$	[32]
Zigana (Gümüşhane)	Dacite	78.7 ± 2.3 75.3 ± 2.4	K-Ar	[25]

Detailed studies on mineral deposits and general geology have been carried out in Demirören (Gümüşhane) region [8, 9, 33, 34], and the studies on the petrology of Late Cretaceous volcanic rocks are limited in this area [8].

In this study, the petrological features of the Late Cretaceous aged Demirören (Gümüşhane) volcanic rocks were revealed, and the development of the Eastern Pontide Late Cretaceous magmatism was tried to be clarified.

2. Regional geology and stratigraphy

The basement rocks of the Eastern Pontides consist of Early Carboniferous metamorphic rocks [35] and Middle to Late Carboniferous plutonic rocks [4, 6, 36–38]. These basement rocks are overlain by the Jurassic volcanics, volcaniclastic and plutonic rocks [39–41]. All these rocks are overlain by Late Jurassic to Early Cretaceous carbonates [42]. The Late Cretaceous series that unconformably overlie carbonate rocks consist of volcanic, plutonic and sedimentary rocks [24, 43–45] and overlain by the Cenozoic units represented by Late Paleocene-Early Eocene adakitic rocks [46, 47], Middle Eocene volcanic, sub-volcanic and sedimentary rocks [2, 3, 23, 45, 48–52], Middle Eocene plutonic rocks [6, 44, 53–57], Neogene volcanic rocks [58], Late Miocene-Pliocene adakitic volcanic-subvolcanic rocks [59]. Quaternary units comprise alluvium and terraces.

The study area is located in the Eastern Pontide Orojenic Belt affected by the Alpine Orogeny. The rock units outcropping in this area were developed in the Mesozoic-Cenozoic period (Figures 1 and 2a). The oldest unit of the study area is the Late Cretaceous volcanics consisting of andesite-basalt and their pyroclasts. The unit is gray black, greenish in color and includes red limestone, sandstone and tuff interlayers in places. The unit was called as the Arduç Formation and aged as Late Cretaceous (Senonian) by [61]. This rock assemblage is most commonly outcropped in the area. On the northwest of the study area, limestones which were named Kapikaya Formation by [61] and aged as Late Cretaceous (Maestrichtian) conformably overlie the Arduç Formation. Limestones reach a thickness of 100 in the area and they are gray, white, yellowish in color, and show partly crystallized. Eocene aged volcano-clastic rock assemblage consisting of andesite-basalt and their pyroclasts unconformably overlies the Late Cretaceous units with the basal conglomerate. The basal conglomerate in the area shows a thickness of 20-30 m in places (Fig. 2b). Within the basal conglomerate, 1-5 cm chert, sedimentary, volcanic and metamorphic rock pebbles are attached with silica and clay cement. These rocks were cut by the Eocene granodiorite-quartz porphyry (Figure 1).

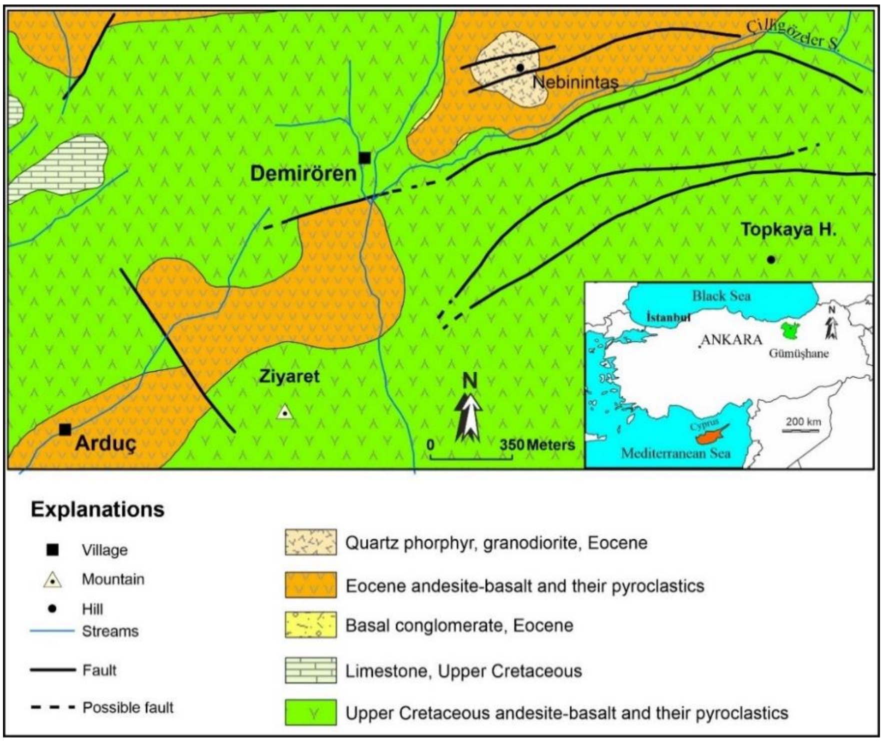

Figure 1. Geological map of the study area (after [60]).

Figure 2. (a) Field view of Late Cretaceous basalt, andesite and their pyroclasts (UKBA: Upper Cretaceous basalt, andesite and their pyroclasts, TK: Basal conglomerate, EG: Eocene granitic rock), (b) Eocene basal conglomerate level and pebbles of different sizes belonging to sedimentary, volcanic and metamorphic rocks

3. Analysis methods

Major, trace and rare earth element (REE) analyzes of six samples that can be used in chemical analyzes as a result of polarizing microscopy examinations were performed in ACME Laboratory (Canada) with Inductively Coupled Plasma Atomic Emission Spectrometer (ICP-AES) and Inductively Coupled Plasma Mass Spectrometer (ICP-MS).

Preparation of the samples for chemical analysis was carried out in the Sample Preparation Laboratory of the Faculty of Engineering and Natural Sciences, Department of Geological Engineering. Rock samples were ground up to 250 mesh with a ring grinder and dried in an oven at 60°C for two days in order to remove their natural moisture, and after stabilization in a desiccator for 24 hours, they were packed in plastic bags. Major, trace element and rare earth element analyzes of the rock samples prepared for analysis were performed in ACME (Canada) laboratories using ICP-MS and ICP-AES. While SO-18/CSC standards were used in the analysis of major oxides, SO-18 standard was used in trace element analysis. For major oxide and trace element analysis, 0.2 g powder sample was mixed with 1.5 g $LiBO_2$ and analyzed after dissolving it in a liquid containing 5% HNO_3, while for rare earth element analysis, 0.250 g powder sample was dissolved in four different acids and analyzed. Major oxides were measured in wt%, trace elements and rare earth elements in ppm. While the detection limits of the main elements vary between 0.001-0.04%, the detection limits of the trace and rare earth elements vary between 0.01-0.5 ppm.

4. Mineralogy and petrography

The Late Cretaceous unit, which consists of basalt-andesite and their pyroclasts, consists of rocks with basaltic andesite, andesite and andesitic tuff character.

Microlithic, microlitic porphyric, porphyric, and partially cumilo phric textures were observed in microscopic examinations. Its main minerals are plagioclase, hornblende, augite, biotite and opaque minerals. Microlithic porphyritic texture is dominant throughout the rock and plagioclases have the largest dimensions (Fig. 3). Plagioclases are mostly euhedral, subhedral, medium and coarse grains and typically show karlsbad twinning with polysynthetic twins. Large crystals usually show a zoned structure. An contents range from 35 to 47. The most common alteration products are calcite, chlorite and clay minerals. Hornblendes were observed as large, euhedral and subhedral prismatic crystals, and as small crystals in groundmass. Some large minerals include plagioclase and opaque mineral inclusions. Same minerals are partially alterated to calcite and opaque minerals. Augites are generally seen as small and medium sized prismatic crystals in some sections. Biotite was observed in small amounts and generally as small prismatic crystals in some sections. Secondary minerals consist of calcite, chlorite, sericite and epidote minerals. Opaque minerals exist as coarse-grained crystals and dispersed. The groundmass is composed of micro and cryptocrystals of plagioclase, hornblende, augite, biotite and opaque mineral grains (Fig. 3).

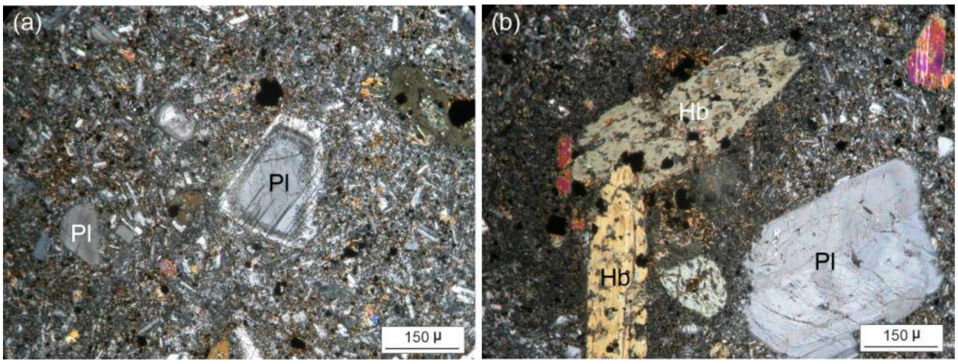

Figure 3. For Demirören volcanic rocks, a) Microlithic porphyric texture in basaltic andesites, b) Porphyric texture in andesites (Crossed Polar, Pl: Plagioclase, Hb: Hornblende)

5. Geochemical properties

The minimum, maximum and average values of the major, trace and rare earth element analyzes of six samples belonging to Demirören volcanic rocks are given in Table 2 and 3. SiO_2 values of Demirören volcanic rocks are in a narrow range, between 53-60%. Basaltic andesites have the lowest (53-55) and the highest SiO_2 contents (58-60) in andesites. The K_2O/Na_2O ratios of the rocks vary between 0.15-1.07, and the magnesium numbers [$Mg\#=100*(MgO/MgO+Fe_2O_3^T)$] vary between 51-59 (Table 2).

Tablo 2. Minimum, maximum and average values of major and trace element analyzes of the Demirören volcanic rocks

Rock	Basaltic andesite			Andesite		
Sample	min	max	avg	min	max	avg
SiO_2	52.66	54.74	53.48	57.65	60.11	59.13
TiO_2	0.59	0.85	0.72	0.41	0.75	0.55
Al_2O_3	16.02	18.06	17.24	11.72	16.21	13.95
Fe_2O_3	7.03	8.70	7.78	5.33	7.36	6.63
MnO	0.08	0.15	0.12	0.08	0.19	0.15
MgO	3.65	4.61	4.28	3.15	3.69	3.44
CaO	6.52	7.77	6.96	5.30	9.45	7.62

Na_2O	3.36	4.28	3.85	2.27	2.66	2.47
K_2O	0.60	1.16	0.94	1.09	2.43	1.76
P_2O_5	0.15	0.26	0.20	0.06	0.11	0.08
LOI	2.40	5.50	4.30	2.60	4.90	3.97
Total	99.81	99.96	99.87	99.45	99.93	99.75
Co	10.80	17.60	15.20	11.00	20.50	16.87
Ni	17.60	26.20	21.00	6.50	26.40	18.87
V	213.00	267.00	231.67	93.00	239.00	182.33
Cu	60.10	102.00	75.40	8.20	79.20	31.93
Pb	6.30	10.80	8.80	7.10	13.90	9.87
Zn	35.00	190.00	88.33	31.00	49.00	42.33
W	0.50	0.50	0.50	0.40	0.50	0.47
Rb	9.00	11.90	10.57	11.00	19.60	14.00
Ba	211.00	486.00	340.67	190.00	341.00	263.67
Sr	395.40	521.80	438.97	276.90	388.10	340.03
Ta	0.20	0.30	0.23	0.10	0.40	0.20
Nb	2.50	3.20	2.80	0.80	1.50	1.07
Hf	2.20	3.00	2.50	1.40	3.00	2.03
Zr	41.20	76.40	62.53	26.70	116.70	62.13
Y	14.50	22.90	18.10	19.60	22.50	20.77
Th	1.90	2.70	2.33	1.50	2.20	1.87
U	0.40	0.80	0.57	0.30	1.10	0.70
Ga	11.50	16.10	14.00	14.40	16.30	15.10
K_2O/Na_2O	0.15	0.32	0.25	0.41	1.07	0.73
Mg #	51.33	58.92	54.70	51.66	56.54	53.56
Sr/Y	22.79	27.57	24.58	14.13	17.58	16.32
Th/Yb	0.96	1.01	0.99	1.09	1.96	1.55
Ce/Pb	2.02	2.49	2.19	1.01	1.61	1.28
Nb/La	0.25	0.41	0.30	0.09	0.29	0.17
La/Nb	2.47	4.00	3.45	3.47	11.63	7.48
Ba/Nb	78.15	194.40	124.70	173.33	426.25	270.23

Mg# (mg-number) = molar 100xMgO/(MgO+ $Fe_2O_3^T$). LOI is loss on ignition

Table 3. Minimum, maximum and average values of rare earth element analyzes of the Demirören volcanic rocks

Rock	**Basaltic andesite**			**Andesite**		
Sample	min	max	avg	min	max	avg
La	7.90	10.80	9.47	5.20	9.30	7.03
Ce	15.70	22.30	18.93	10.60	14.10	12.03
Pr	2.14	3.06	2.56	1.51	1.95	1.67
Nd	10.40	13.90	11.67	7.20	9.60	8.17
Sm	2.31	3.39	2.71	2.16	2.86	2.55
Eu	1.04	1.17	1.11	0.63	0.72	0.69
Gd	2.75	3.19	2.93	1.74	2.42	2.15
Tb	0.49	0.69	0.62	0.30	0.38	0.34
Dy	3.37	4.40	3.92	2.04	2.79	2.49
Ho	0.69	0.99	0.85	0.39	0.53	0.44
Er	1.92	2.69	2.36	1.12	1.47	1.32
Tm	0.30	0.41	0.36	0.17	0.22	0.19
Yb	1.89	2.70	2.36	1.12	1.38	1.23
Lu	0.34	0.40	0.37	0.19	0.22	0.20
$(Eu/Eu^*)_n$	1.03	1.42	1.22	0.82	0.97	0.88
$(La/Lu)_n$	2.21	2.95	2.65	2.45	5.07	3.64
$(La/Sm)_n$	2.01	2.51	2.22	1.52	2.05	1.71
$(Gd/Lu)_n$	0.92	1.04	0.98	1.08	1.50	1.31
$(La/Yb)_n$	2.14	3.47	2.77	2.55	5.61	3.97

$Eu^*=(Sm+Gd)_n/2$

In the SiO_2 versus (Na_2O+K_2O) diagram [63], Demirören volcanic rocks are in the composition of basaltic andesite and andesite with subalkaline character (Fig. 4a). In the SiO_2-Zr/TiO_2 diagram [64], the samples consist of andesite and basalt composition rocks (Fig. 4b).

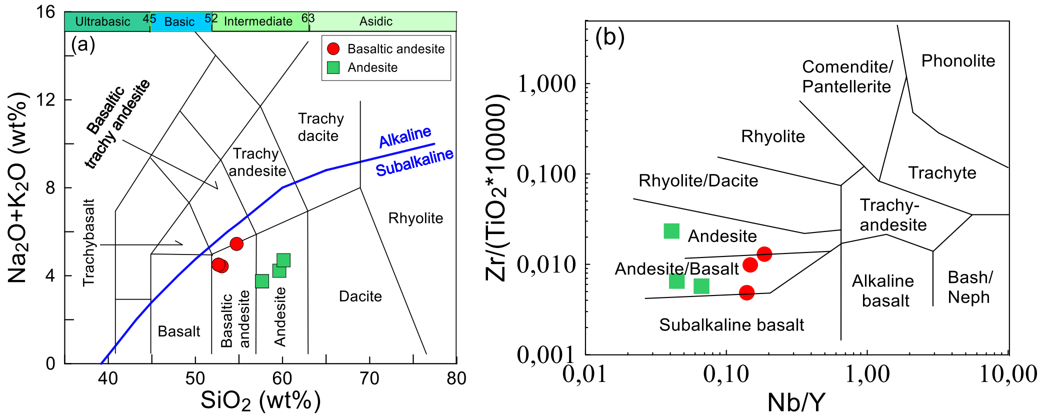

Figure 4. For Demirören volcanic rock samples a) SiO_2 versus total alkali (Na_2O+K_2O) diagram [63] b) SiO_2 versus Zr/TiO_2 classification diagram [64] (Alkali/subalkaline separation curve taken from [65])

In the Th-Co diagram [66], all of the samples are of calc-alkaline character (Fig. 5a). Rock samples have medium-high potassium content in the K_2O-SiO_2 diagram [63](Fig. 5b).

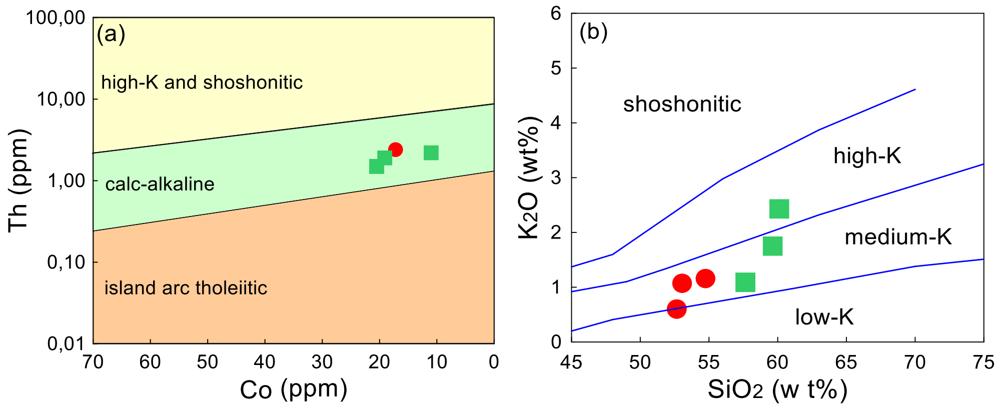

Figure 5. For Demirören volcanic rocks, a) Th-Co diagram [66], b) SiO_2 vs. K_2O diagram (The field boundaries between medium-K, high-K and shoshonitic are from [67]).

The rocks also show calc-alkaline character according to the AFM diagram (Fig. 6).

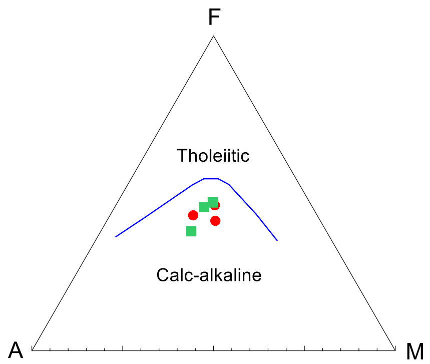

Figure 6. The positions of the samples of the Demirören volcanic rocks in the AFM diagram (Tholeitic-calc alkali separation curve taken from [65]).

In the SiO_2 versus major element variation diagrams, as SiO_2 values increase, CaO, MgO, Al_2O_3, $Fe_2O_3^T$, TiO_2 and P_2O_5 values decrease while K_2O values increase (Figure 7).

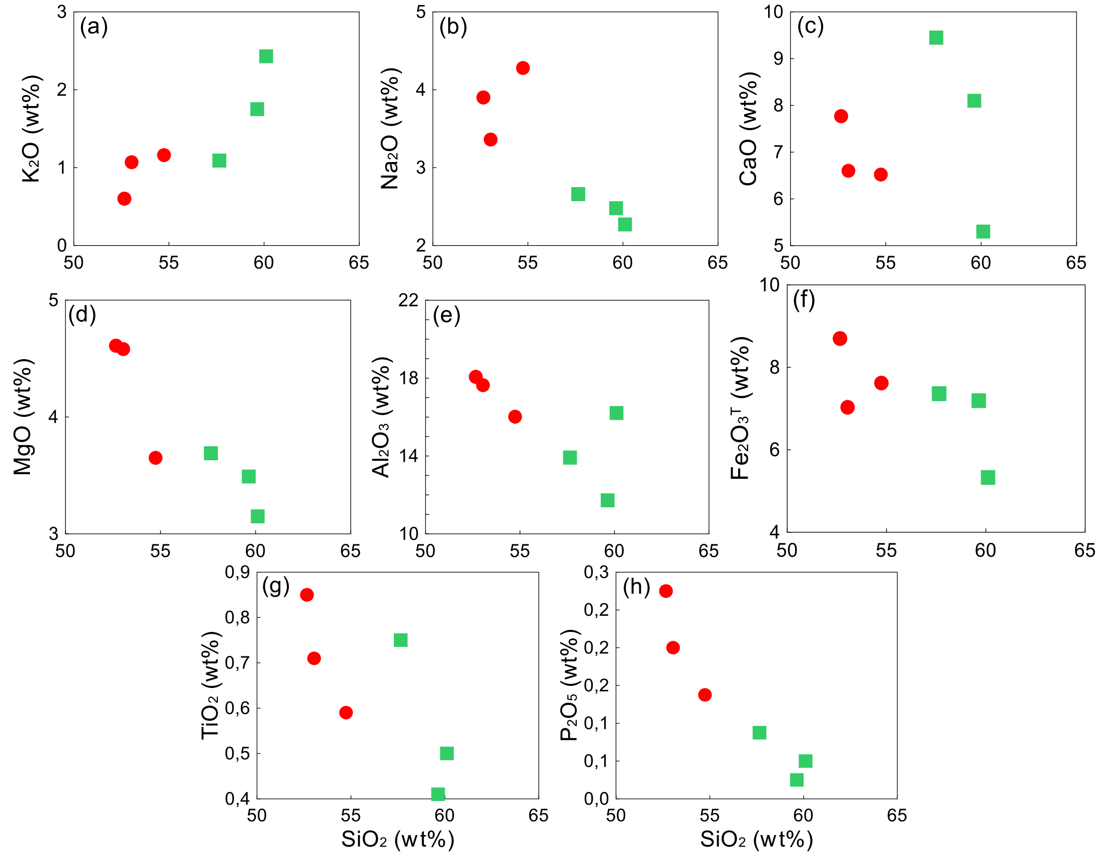

Figure 7. SiO_2 versus major element variation diagrams of Demirören volcanic rocks samples

In the trace element variation diagrams against SiO_2, as SiO_2 increases, a positive correlation is observed for Rb and Pb values, while a negative relationship is observed for Ba, Sr, Th, Ni, Y and Nb values (Figure 8).

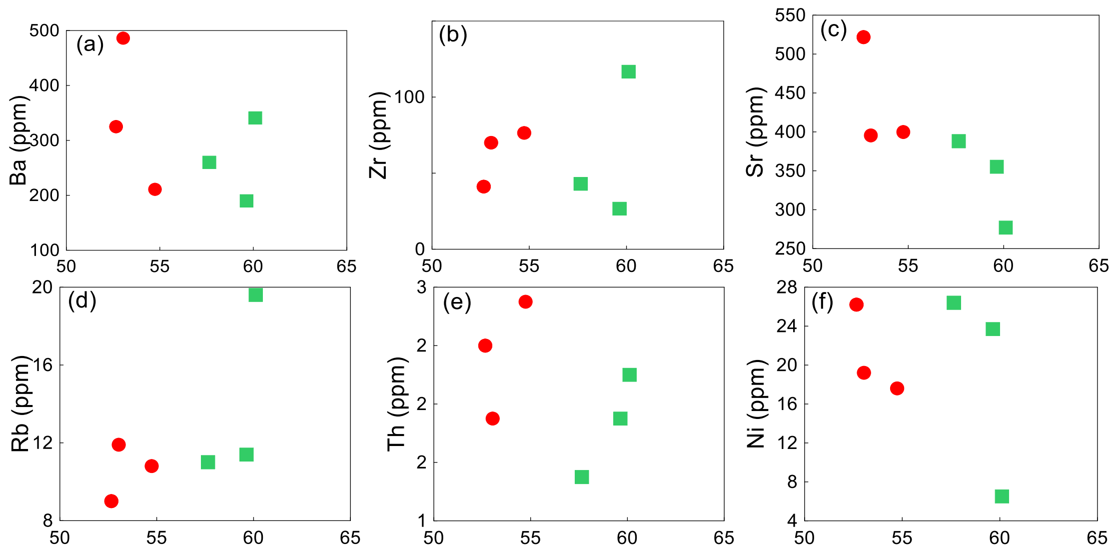

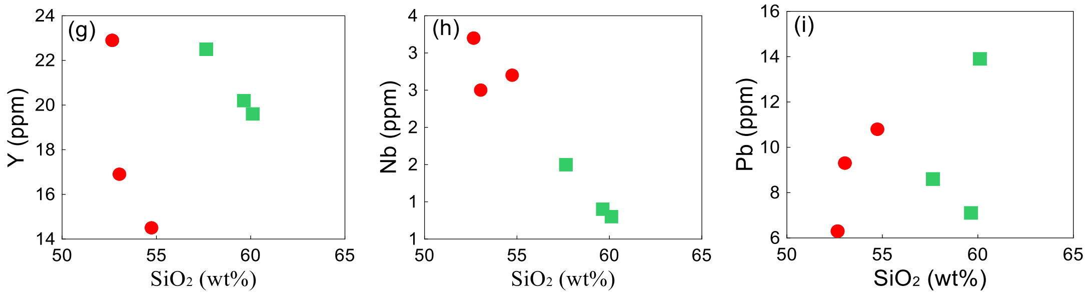

Figure 8. Trace element variation diagrams against SiO_2 of the Demirören volcanic rocks

In primitive mantle-normalized trace element variation diagrams [68] of the samples are given in Fig. 9. While enrichment is observed in the samples in terms of incompatible elements, depletion is observed in terms of compatible elements such as Ti, Nb and Ta (Fig. 9). The negative Nb and Ta anomaly indicates that the subduction component plays an active role in the development of the main magma of the rocks.

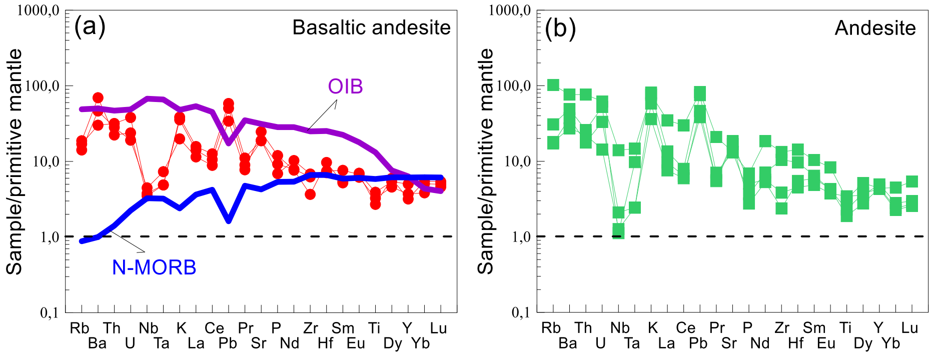

Figure 9. (a-b) Primitive mantle-normalized trace element variation diagrams [68] of the Demirören volcanic rocks

The rare earth element (REE) distributions of the investigated volcanic rocks, normalized to chondrite [69], are given in Fig. 10 and seen that all samples are generally similar to each other (Fig. 10). This indicates that the rocks forming the volcanic rocks in the study area are derived from a similar mantle source. In the chondrite-normalized rare earth element variation diagrams of the studied volcanic rocks (Figure 10), light rare earth elements (LREEs) are more enriched than heavy rare earth elements (HREEs). While the $(La/Lu)_N$ ratios of the samples varied between 2.21 and 5.07, the $(Gd/Lu)_N$ ratios varied between 0.92 and 1.50 (Table 2). Basaltic andesite samples show positive (Eu/Eu*)n anomalies (1.03 to 1.42), while andesite samples show negative (Eu/Eu*)n anomalies (0.82 to 0.97) (Table 2, Figure 10).

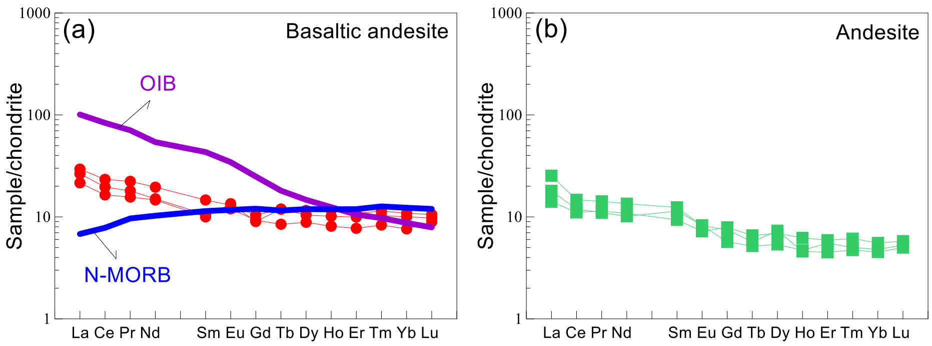

Figure 10. (a-b) Rare earth element normalized to chondrite variation diagrams of the Demirören volcanic rocks [69]

According to the Nb/Th versus Nb tectonic discrimination diagram (Fig. 11a), the samples fall into the arc volcanic area and nearby. The Sr/Y ratios of the rocks are between 14 and 28, and the samples are located in the normal arc volcanic series area in the Sr/Y vs. Y discrimination diagram [70] (Figure 11b).

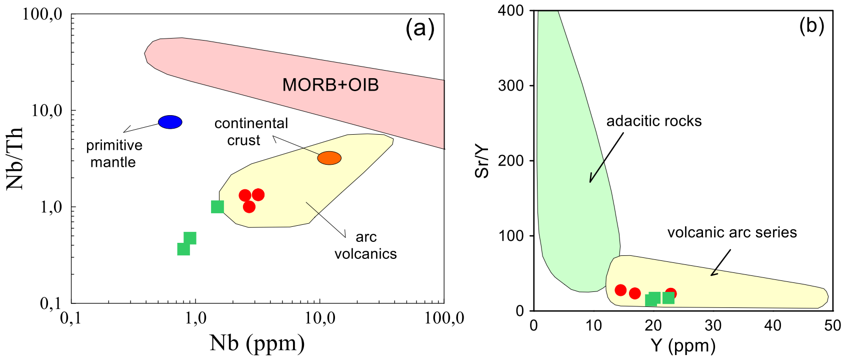

Figure 11. Tectonic discrimination diagrams of the Demirören volcanic rocks. (a) Nb/Th vs. Nb diagram (primary mantle values from [71], continental basalt-MORB+OIB and volcanic arc areas from [72]). (b) Sr/Y vs. Y discrimination diagram [70]

6. Discussion

The MgO values vary between 1.8-7.4%, Mg numbers (Mg#) between 36-67 and Ni values between 2-49 (ppm) of the the Demirören volcanic rocks. These values indicate that the Demirören volcanic rocks differ significantly from magmas derived from the primitive mantle composition (Mg# = ~ 66 to 75, Ni = ~ 400 to 500 ppm; [73]).

The distribution pattern of the some major and trace elements of the studied Demirören samples (Figures 7 and 8) support plagioclase + hornblende ± pyroxene + Fe-Ti oxide fractionations.

In the Y versus Rb diagram (Fig. 12a), Late Cretaceous volcanic rocks have a low-Y series trend, indicating that plagioclase and hornblende fractionation is effective in the rocks. The Sr versus MgO diagram (Fig. 12b) indicates fractionation of ferro-magnesian minerals.

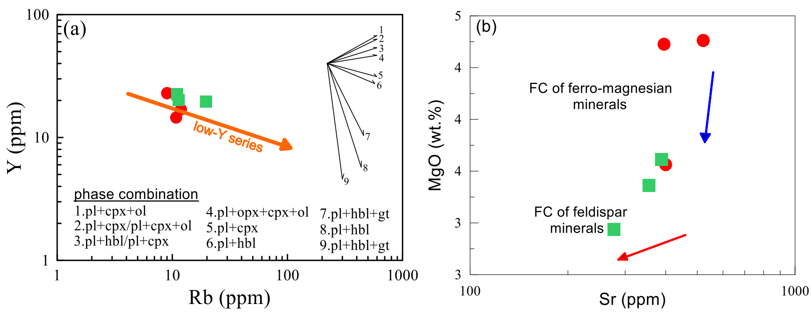

Figure 12. For the Demirören volcanic rocks (a) Y (ppm) versus Rb (ppm) diagram (b) MgO versus Sr diagram

Low $(La/Yb)_N$ ratios (2.4-10.6) and high Th/Yb ratios (0.4-8.6) (Table 2 and 3), as well as enrichment of LILE and LREEs and negative Nb and Ta anomalies (Figure 7) of the studied samples indicate subduction-related metasomatised mantle source [74].

Ba/Th vs. La/Sm and Sr/La vs. La/Yb diagrams (Figure 13 a and b) show that the melt was enriched in the fluids [75] during the Late Cretaceous subduction.

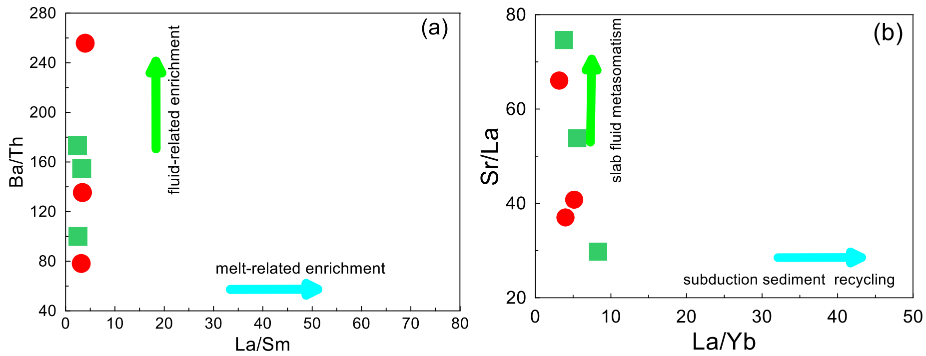

Figure 13. For the Demirören volcanic rocks (a) Ba/Th versus La/Sm diagram and (b) Sr/La versus La/Yb diagram

In the Ce/Pb vs. Ce diagram (Fig. 14a), the samples of the studied volcanic rocks are located in the arc volcanics area. The low Ce/Pb ratios observed in the samples (1.01 to 2.49) differ from oceanic basalts (20 to 30) [71], indicating that the studied volcanic rocks did not derive from an asthenospheric mantle source. Nb/La ratios are useful in determining the partial melting point and source composition of volcanic rocks [76]. Low Nb/La ratios (<0.5) indicate a lithospheric mantle source, and high Nb/La ratios (>1) indicate an ocean island basalt (OIB)-like asthenospheric mantle source [77]. The Nb/La ratios of the studied volcanic rocks range from 0.09 to 0.41 (Table 2), indicating a spinel lerzolithic lithospheric mantle source (Figure 14b).

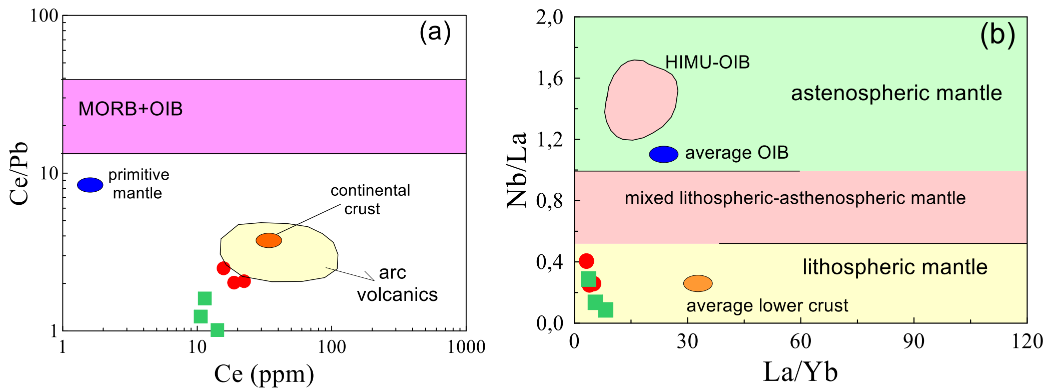

Figure 14. For the Demirören volcanic rocks; (a) Ce/Pb vs. Ce diagram, (b) Nb/La vs. La/Yb diagram. For reference values in diagrams, see Figure 9 caption in [49].

The studied volcanic rocks are located in the arc volcanics area (Fig. 11). La/Nb and Ba/Nb ratios of volcanic rocks indicated that the source of these volcanic rocks is related subduction zone enrichment. At the time of subduction, LILE and LREE elements are transported upwards via fluids derived from the slab [78]. Significant LILE and LREE enrichments observed in the studied volcanics indicate an enriched mantle source rather than a depleted mantle source [79]

7. Conclusions

1. The studied Demirören volcanic rocks are basaltic andesite and andesite in composition defining a calc-alkaline series.
2. All of the samples display similar geochemical features characterized by enrichment in large-ion lithofile elements (LILEs) and light rare earth elements (LREEs), with pronounced depletion in high-field-strength elements (HFSEs) indicating similar sources and petrogenetic processes.
3. The main solidification processes involved in the evolution of the volcanic rocks consist of fractional crystallization (FC).
4. Plagioclase, hornblende, pyroxene and Fe-Ti oxides are the most important fractionating mineral phases.
5. The studied volcanic rocks were derived from a subcontinental lithospheric mantle (SCLM), whih was enriched by fluids in a subduction-related geodynamic setting.

Acknowledgement

This study was financially supported by Gümüşhane University Scientific Research Projects Unit (GUBAP Proje No: 13.F5114.02.08). Authors thank the editors and anonymous referees for their contributions during the review and evaluation phase of the article.

References

[1] Kaygusuz A, Arslan M, Temizel İ, Yücel C, Aydınçakır E. U–Pb zircon ages and petrogenesis of the Late Cretaceous I-type granitoids in arc setting, Eastern Pontides, NE Turkey. Journal of African Earth Sciences 2021; 174:104040.

[2] Arslan M, Temizel I, Abdioğlu E, Kolayli H, Yücel C, Boztuğ D, Şen C. 40Ar-39Ar dating, whole-rock and Sr-Nd-Pb isotope geochemistry of post-collisional Eocene volcanic rocks in the southern part of the Eastern Pontides (NE Turkey): Implications for magma evolution in extension-induced origin. Contributions to Mineralogy and Petrology 2013; 166:113–142.

[3] Aslan Z, Arslan M, Temizel I, Kaygusuz A. K-Ar dating, whole-rock and Sr-Nd isotope geochemistry of calc-alkaline volcanic rocks around the Gümüşhane area: Implications for post-collisional volcanism in the Eastern Pontides, Northeast Turkey. Mineralogy and Petrology 2014; 108:245–267.

[4] Vural A, Kaygusuz A. Petrology of the Paleozoic Plutons in Eastern Pontides: Artabel Pluton (Gümüşhane, NE Turkey). Journal of Engineering Research and Applied Science 2019; 8:1216–1228.

[5] Temizel İ, Arslan M, Yücel C, Yazar EA, Kaygusuz A, Aslan Z. U-Pb geochronology, bulk-rock geochemistry and petrology of Late Cretaceous syenitic plutons in the Gölköy (Ordu) area (NE Turkey): Implications for magma generation in a continental arc extension triggered by slab roll-back. Journal of Asian Earth Sciences 2019; 171:305–320.

[6] Temizel I, Arslan M, Yücel C, Abdioğlu Yazar E, Kaygusuz A, Aslan Z. Eocene tonalite–granodiorite from the Havza (Samsun) area, northern Turkey: adakite-like melts of lithospheric mantle and crust generated in a post-collisional setting. International Geology Review 2020; 62:1131–1158.

[7] Sipahi F, Saydam Eker Ç, Akpınar İ, Gücer MA, Vural A, Kaygusuz A, Aydurmuş T. Eocene magmatism and associated Fe-Cu mineralization in northeastern Turkey: a case study of the Karadağ skarn. International Geology Review 2021:1–26.

[8] Vural A, Akpınar İ, Kaygusuz A, Sipahi F. Petrological characteristics of Eocene volcanic rocks around Demirören (Gümüşhane, NE Turkey). Journal of Engineering Research and Applied Science 2021; 10:1703–1716.

[9] Vural A, Sipahi F. Demirören (Gümüşhane) Fe-skarn yatağının Jeolojik, Jeokimyasal ve kayaç kimyası, köken özellikleri açısından incelenmesi. Gümüşhane, Türkiye: 2016.

[10] Sipahi F, Akpınar İ, Saydam Eker Ç, Kaygusuz A, Vural A, Yılmaz M. Formation of the Eğrikar (Gümüşhane) Fe–Cu skarn type mineralization in NE Turkey: U–Pb zircon age, lithogeochemistry, mineral chemistry, fluid inclusion, and O-H-C-S isotopic compositions. Journal of Geochemical Exploration 2017; 182:32–52.

[11] Vural A. Evaluation of soil geochemistry data of Canca Area (Gümüşhane, Turkey) by means of Inverse Distance Weighting (IDW) and Kriging methods-preliminary findings. Bulletin Of The Mineral Research and Exploration 2018; 158:10–20.

[12] Vural A, Erdoğan M. Eski Gümüşhane Kırkpavli Alterasyon Sahasında Toprak Jeokimyası. Gümüşhane Üniversitesi Fen Bilimleri Enstitüsü Dergisi 2014; 4:1–15.

[13] Vural A, Ersen F. Geology, mineralogy and geochemistry of manganese mineralization in Gumushane, Turkey. Journal of Engineering Research and Applied Science 2019; 8:1051–1059.

[14] Çamur MZ, Güven İH, Er M. Geochemical characteristics of the eastern Pontide volcanics: an example of multiple volcanic cycles in arc evolution. Turkish Journal of Earth Sciences 1996:123–144.

[15] Arslan M, Tüysüz N, Korkmaz S, Kurt H. Geochemistry and petrogenesis of the eastern Pontide volcanic rocks, Northeast Turkey. Chemie Der Erde Geochemistry 1997; 57:157–187.

[16] Özsayar T, Pelin S, Gedikoğlu A. Doğu Pontidlerde Kretase. KTÜ Yer Bilimleri Dergisi 1981; 1:65–114.

[17] Boztuğ D, Erçin AI, Kuruçelik MK, Göç D, Kömür I, Iskenderoğlu A. Geochemical

characteristics of the composite Kaçkar batholith generated in a Neo-Tethyan convergence system, Eastern Pontides, Turkey. Journal of Asian Earth Sciences 2006; 27:286–302.

[18] Kaygusuz A, Siebel W, Şen C, Satir M. Petrochemistry and petrology of I-type granitoids in an arc setting: The composite Torul pluton, Eastern Pontides, NE Turkey. International Journal of Earth Sciences 2008; 97:739–764.

[19] Karslı O, Dokuz A, Uysal I, Aydin F, Chen B, Kandemir R, Wijbrans J. Relative contributions of crust and mantle to generation of Campanian high-K calc-alkaline I-type granitoids in a subduction setting, with special reference to the Harşit Pluton, Eastern Turkey. Contributions to Mineralogy and Petrology 2010; 160:467–487.

[20] Eyuboglu Y, Santosh M, Bektas O, Ayhan S. Arc magmatism as a window to plate kinematics and subduction polarity: Example from the eastern Pontides belt, NE Turkey. Geoscience Frontiers 2011; 2:49–56.

[21] Aydınçakır E, Kaygusuz A. Geç Kretase Yaşlı Dağbaşı (Araklı, Trabzon) Volkanitlerinin Petrografik ve Jeokimyasal Özellikleri, KD Türkiye. Gümüşhane Üniversitesi, Fen Bilimleri Enstitüsü Dergisi 2012; 2:123–142.

[22] Özdamar Ş. Geochemistry and geochronology of late Mesozoic volcanic rocks in the northern part of the Eastern Pontide Orogenic Belt (NE Turkey): Implications for the closure of the Neo-Tethys Ocean. Lithos 2016; 248–252:240–256.

[23] Yücel C, Arslan M, Temizel İ, Abdioğlu Yazar E, Ruffet G. Evolution of K-rich magmas derived from a net veined lithospheric mantle in an ongoing extensional setting: Geochronology and geochemistry of Eocene and Miocene volcanic rocks from Eastern Pontides (Turkey). Gondwana Research 2017; 45:65–86.

[24] Aydin F, Dokuz A, Kandemir R, Karsli O. Temporal, geochemical and geodynamic evolution of the Late Cretaceous subduction zone volcanism in the eastern Sakarya Zone , NE Turkey : implications for mantle-crust interaction in an arc setting 2020.

[25] Sipahi F. Zigana Dağı (Torul–Gümüşhane) Volkanitlerindeki Hidrotermal Ayrışmaların Mineraloji ve Jeokimyası. Karadeniz Teknik Üniversitesi, Trabzon, Türkiye, 2005.

[26] Kaygusuz A, Saydam Eker Ç. Geochemical features and petrogenesis of Late Cretaceous subduction-related volcanic rocks in the Değirmentaşı (Torul/Gümüşhane) area, Eastern Pontides (NE Turkey). Journal of Engineering Research and Applied Science 2021; 10:1689–1702.

[27] Kandemir Ö, Akbayram K, Çobankaya M, Kanar F, Pehlivan Ş, Tok T, Hakyemez A, Ekmekçi E, Danacı F, Temiz U. From arc evolution to arccontinent collision: Late Cretaceous–middle Eocene geology of the Eastern Pontides, northeastern Turkey. Geological Society of America Bulletin 2019; 131:1889–1906.

[28] Alan İ, Balcı V, Keskin H, Altun İ, Böke N, Demirbağ H, Arman S, Elibol H, Soyakıl M, Kop A, Hanilçi N. Tectonostratigraphic characteristics of the area between Çayeli (Rize) and İspir (Erzurum). Bulletin of the Mineral Research and Exploration 2019; 158:1–29.

[29] Yücel C. Akçaabat (Trabzon) Güneyi ve Çevresindeki Kampaniyen Yaşlı Volkanik Kayaçların Petrografisi, Jeokimyası, Jeokronolojisi ve Petrojenezi. Gümüşhane Üniversitesi, Fen Bilimleri Enstitüsü Dergisi 2017; 7:79–101.

[30] Eyuboglu Y. Petrogenesis and U–Pb zircon chronology of felsic tuffs interbedded with turbidites (Eastern Pontides Orogenic Belt, NE Turkey): Implications for Mesozoic geodynamic evolution of the eastern Mediterranean region and accumulation rates of turbidite sequenc. Lithos 2015; 212–215:74–92.

[31] Eyuboglu Y, Santosh M, Yi K, Tuysuz N, Korkmaz S, Akaryali E, Dudas FO, Bektas O. The Eastern Black Sea-type volcanogenic massive sulfide deposits: Geochemistry, zircon U-Pb geochronology and an overview of the geodynamics of ore genesis. Ore Geology Reviews 2014; 59:29–54.

[32] Eyüboğlu Y. Late Cretaceous high-K volcanism in the eastern Pontide orogenic belt: Implications for the geodynamic evolution of NE Turkey. vol. 52. 2010.

[33] Vural A. Investigation of the radiation risk to the inhabitants in the region close to the hydrothermal alteration site, Gümüşhane/Turkey. Journal of Engineering Research and Applied Science 2019; 8:1168–1176.

[34] Sungur A, Vural A, Gundogdu A, Soylak M. Effect of antimonite mineralization area on heavy metal contents and geochemical fractions of agricultural soils in Gümüşhane Province, Turkey. Catena 2020; 184:104255.

[35] Topuz G, Altherr R, Kalt A, Satir M, Werner O, Schwarz WH. Aluminous granulites from the Pulur complex, NE Turkey: A case of partial melting, efficient melt extraction and crystallisation. Lithos 2004; 72:183–207.

[36] Topuz G, Altherr R, Siebel W, Schwarz WH, Zack T, Hasözbek A, Barth M, Satır M, Şen C. Carboniferous high-potassium I-type granitoid magmatism in the Eastern Pontides: The Gümüşhane pluton (NE Turkey). Lithos 2010; 116:92–110.

[37] Kaygusuz A, Arslan M, Siebel W, Sipahi F, Ilbeyli N. Geochronological evidence and tectonic significance of Carboniferous magmatism in the southwest Trabzon area, eastern Pontides, Turkey. International Geology Review 2012; 54:1776–1800.

[38] Kaygusuz A, Arslan M, Sipahi F, Temizel İ. U-Pb zircon chronology and petrogenesis of Carboniferous plutons in the northern part of the Eastern Pontides, NE Turkey: Constraints for Paleozoic magmatism and geodynamic evolution. Gondwana Research 2016; 39:327–346.

[39] Dokuz A, Karsli O, Chen B, Uysal I. Sources and petrogenesis of Jurassic granitoids in the Yusufeli area, Northeastern Turkey: Implications for pre- and post-collisional lithospheric thinning of the eastern Pontides. Tectonophysics 2010; 480:259–279.

[40] Saydam Eker C, Sipahi F, Kaygusuz A. Trace and rare earth elements as indicators of provenance and depositional environments of Lias cherts in Gumushane, NE Turkey. Chemie Der Erde - Geochemistry 2012; 72:167–177.

[41] Eyuboğlu Y, Dudas FO, Santosh M, Zhu DC, Yi K, Chatterjee N, Akaryalı E, Liu Z. Cenozoic forearc gabbros from the northern zone of the Eastern Pontides Orogenic Belt, NE Turkey: implications for slab window magmatism and convergent margin tectonics. Gondwana Research 2016; 33:160–190.

[42] Pelin S. Geological study of the area southeast of Alucra (Giresun) with special reference to its petroleum potential. Trabzon, Türkiye: Karadeniz Teknik Üniversitesi Yayın No. 87; 1977.

[43] Aydınçakır E. Subduction-related Late Cretaceous high-K volcanism in the Central Pontides orogenic belt: Constraints on geodynamic implications. Geodinamica Acta 2016; 28:379–411.

[44] Temizel İ, Abdioğlu Yazar E, Arslan M, Kaygusuz A, Aslan Z. Mineral chemistry, whole-rock geochemistry and petrology of Eocene I-type shoshonitic plutons in the Gölköy area (Ordu, NE Turkey). Bulletin of the Mineral Research and Exploration 2018; 157:121–152.

[45] Kaygusuz A, Gucer MA, Yucel C, Aydincakir E, Sipahi F. Petrography and crystallization conditions of Middle Eocene volcanic rocks in the Aydıntepe -Yazyurdu (Bayburt) area , Eastern Pontides (NE Turkey). Journal of Engineering Research and Applied Science 2019; 8:1205–1215.

[46] Topuz G, Okay AI, Altherr R, Schwarz WH, Siebel W, Zack T, Satir M, Sen C. Post-collisional adakite-like magmatism in the Agvanis Massif and implications for the evolution of the Eocene magmatism in the Eastern Pontides (NE Turkey). Lithos 2011; 125:131–150.

[47] Eyuboglu Y, Dudas FO, Santosh M, Yi K, Kwon S, Akaryali E. Petrogenesis and U-Pb zircon chronology of adakitic porphyries within the Kop ultramafic massif (Eastern Pontides Orogenic Belt, NE Turkey). Gondwana Research 2013; 24:742–766.

[48] Tokel S. Doğu Karadeniz bölgesinde Eosen yaşlı kalkalkalen andezitler ve jeotektonizma. Türkiye Jeoloji Kurultayı Büllteni 1977; 20:49–54.

[49] Kaygusuz A, Arslan A, Siebel W, Şen C. Geochemical and Sr-Nd Isotopic Characteristics of Post-Collisional Calc-Alkaline Volcanics in the Eastern Pontides (NE Turkey). Turkish Journal of Earth Sciences 2011; 20:137–159.

[50] Kaygusuz A, Merdan-Tutar Z, Yucel C. Mineral chemistry, crystallization conditions and petrography of Cenozoic volcanic rocks in the Bahçecik (Torul/Gumushane) area, Eastern Pontides (NE Turkey). Journal of Engineering Research and Applied Science 2017; 6:641–651.

[51] Temizel I, Arslan M, Ruffet G, Peucat JJ. Petrochemistry, geochronology and Sr-Nd isotopic systematics of the Tertiary collisional and post-collisional volcanic rocks from the Ulubey (Ordu) area, eastern Pontide, NE Turkey: Implications for extension-related origin and mantle source characteristics. Lithos 2012; 128–131:126–147.

[52] Kaygusuz A, Sahin K. Petrographical , geochemical and petrological characteristics of Eocene volcanic rocks in the Mescitli area , Eastern Pontides (NE Turkey). Journal of Engineering Research and Applied Science 2016; 5:473–486.

[53] Karslı O, Chen B, Aydin F, Şen C. Geochemical and Sr-Nd-Pb isotopic compositions of the Eocene Dölek and Sariçiçek Plutons, Eastern Turkey: Implications for magma interaction in the genesis of high-K calc-alkaline granitoids in a post-collision extensional setting. Lithos 2007; 98:67–96.
[54] Kaygusuz A, Öztürk M. Geochronology, geochemistry, and petrogenesis of the Eocene Bayburt intrusions, Eastern Pontide, NE Turkey: implications for lithospheric mantle and lower crustal sources in the high-K calc-alkaline magmatism. Journal of Asian Earth Sciences 2015; 108:97–116.
[55] Vural A, Kaygusuz A. Geochronology, petrogenesis and tectonic importance of Eocene I-type magmatism in the Eastern Pontides, NE Turkey. Arabian Journal of Geosciences 2021; 14:467.
[56] Kaygusuz A, Yücel C, Arslan M, Sipahi F, Temizel İ, Çakmak G, Güloğlu ZS. Petrography, mineral chemistry and crystallization conditions of Cenozoic plutonic rocks located to the north of Bayburt (Eastern Pontides, Turkey). Bulletin of the Mineral Research and Exploration 2018; 157:75–102.
[57] Kaygusuz A, Yücel C, Arslan M, Temizel İ, Yi K, Jeong Y-J, Siebel W, Sipahi F. Eocene I-type magmatism in the Eastern Pontides, NE Turkey: Insights into magma genesis and magma-tectonic evolution from whole-rock geochemistry, geochronology and isotope systematics. International Geology Review 2020.
[58] Aydin F, Karslı O, Chen B. Petrogenesis of the Neogene alkaline volcanics with implications for post-collisional lithospheric thinning of the Eastern Pontides, NE Turkey. Lithos 2008; 104:249–266.
[59] Yücel C. Geochronology, geochemistry, and petrology of adakitic Pliocene–Quaternary volcanism in the Şebinkarahisar (Giresun) area, NE Turkey. International Geology Review 2019; 61:754–777.
[60] Vural A. Demirören/Gümüşhane-Türkiye Kuvars Porfiri Kayacı ve İlişkili Skarn-Metasomatizmanın Jeokimyasal Özellikleri. Euroasia Journal of Mathematics, Engineering, Natural and Medical Sciences 2020; 7:97–121.
[61] Keskin İ, Korkmazer S, Gedik İ. Bayburt Dolayının Jeolojisi. Ankara, Türkiye: 1989.
[62] Güven İ. Doğu Pontidlerin 1/25000 Ölçekli Kompilasyonu. Ankara: MTA Genel Müdürlüğü; 1993.
[63] Le Maitre RW, Bateman P, Dudek A, Keller J, Lameyre J, Le Bas MJ, Sabine PA, Schmid R, Sorensen H, Streckeisen A, Woolley AR, Zanettin B. A Classification of Igneous Rocks and Glossary of Terms: Recommendations of the International Union of Geological Sciences Subcommission on the Systematics of Igneous rocks. Blackwell Scientific Publications, Oxford, U.K.; 1989.
[64] Winchester JA, Floyd PA. Geochemical discrimination of different magma series and their differentiation products using immobile elements. Chemical Geology 1977; 20:325–343.
[65] Irvine TN, Baragar WRA. A guide to the chemical classification of the common volcanic rocks. Canadian Journal of Earth Sciences 1971; 8:523–548.
[66] Le Maitre RW, Streckeisen A, Zanettin B, Le Bas MJ, Bonin B, Bateman P, Bellieni G, Dudek A, Efremova S, Keller J, Lamere J, Sabine PA, et al. Igneous rocks: A classification and glossary of terms, recommendations of the international union of geological sciences, subcommission of the systematics of igneous rocks. Cambridge: Cambridge University Press; 2002.
[67] Peccerillo A, Taylor SR. Geochemistry of eocene calc-alkaline volcanic rocks from the Kastamonu area, Northern Turkey. Contributions to Mineralogy and Petrology 1976; 58:63–81.
[68] Sun SS, McDonough WF. Chemical and isotopic systematics of oceanic basalts: Implications for mantle composition and processes. Geological Society Special Publication 1989; 42:313–345.
[69] Taylor SR, McLennan SM. The Continental Crust; its Composition and Evolution Geoscience Text. Blackwell Scientific Publications, Oxford, U.K.; 1985.
[70] Drummond MS, Defant M. J. A model for trondhjemite-tonalite-dacite genesis and crustal growth via slab melting: Archean to modern comparisons. Journal of Geophysical Research 1990; 95:21503–21521.
[71] Hoffmann AW. Chemical differentiation of the Earth. The relationship between mantle, continental crust and oceanic crust. Earth and Planetary Science Letters 1988; 90:297–314.
[72] Schmidberger SS, Hegner E. Geochemistry and isotope ststematics of calc-alkaline volcanic rocks from the Saar-Nahe basin (SW Germany)-implications for Late Variscan orogenic development. Contributions to Mineralogy and Petrology 1999; 135:373–385.

[73] Frey FA, Green D, Roy S. Integrated models of basalt of petrogenesis, a study of quartz tholeiites to olivine melilitites from south Australia utilizing geochemical and experimental petrological data. Journal of Petrology 1978; 19:463–513.

[74] Pearce JA, Peate DW. Tectonic implications of the composition of volcanic arc magmas. Annual Review of Earth and Planetary Sciences 1995; 23:251–285.

[75] Guo F, Li H, Fan W, Li J, Zhao L, Huang M, Xu W. Early Jurassic subduction of the Paleo-Pacific Ocean in NE China: Petrologic and geochemical evidence from the Tumen mafic intrusive complex. Lithos 2015; 224–225:46–60.

[76] Jahn BM, Wu FY, Lo CH. Crust-mantle interaction induced by deep subduction of the continental crust: geochemical and Sr-Nd isotopic evidence from post-collisional mafic-ultramafic intrusions of the northern Dabie Complex, Central China. Chemical Geology 1999; 157:119–146.

[77] Smith EI, Sanchez A, Walker JD, Wang K. Geochemistry of mafic magmas in the Hurricane Volcanic field, Utah: implications for small- and large-scale chemical variability of the lithospheric mantle. Journal of Geology 1999; 107:433–448.

[78] Elburg MA, Bergen MV, Hoogewerff J, Foden J, Vroon P, Zulkarnain I, Nasution A. Geochemical trends across an arc-continent collision zone: magma sources and slab-wedge transfer processes below the Pantar Strait volcanoes, Indonesia. Geochimica et Cosmochimica Acta 2002; 66:2771–2789.

[79] Condie KC, Frey BA, Kerrich R. The 1.75-Ga Iron King Volcanics in westcentral Arizona: a remnant of an accreted oceanic plateau derived from a mantle plume with a deep depleted component. Lithos 2002; 64:49–62..

..